Sorption of Bisphenol A in Aqueous Solutions on Irradiated and as-Grown Multiwalled Carbon Nanotubes

RALUCA MADALINA SENIN[1,2], ION ION[2], OVIDIU OPREA[2], RUSANDICA STOICA[1], RODICA GANEA[1], ALINA CATRINEL ION[2]*

[1]National Research & Development Institute for Chemistry and Petrochemistry ICECHIM, 202 Splaiul Independentei, 060021, Bucharest, Romania

[2]University Polkitehnica of Bucharest, 313 Splaiul Independentei , 060042, Romania

In this study, non-irradiated and weathered multiwalled carbon nanotubes (MWCNTs) obtained through irradiation, were studied as adsorbents for BPA, both nanomaterials being characterized before and after the adsorption process. The objectives of our investigation were to compare the characteristics of non-irradiated and irradiated MWCNTs, to evaluate the adsorption capacity of BPA by pristine and irradiated MWCNTs and to determine the variation of the kinetic, sorption and thermodynamic parameters during sorption process using both sorbents.

Keywords: sorption, bisphenol A, carbon nanomaterials, environment

Endocrine disrupting chemicals (EDC) might have serious effects in the living bodies especially over the endocrine glands [1], this why their removal being important for environmental protection. Bisphenol A (BPA) has been reported in the environment, in rivers, seas and soils, being used in the production of polycarbonate and epoxy resins. It presents several risks to humans and to animals, this why its removal from the environmental matrices being intensively studied in the last years [2]. Especially in water treatment, adsorption is largely used for removing several organic [3] and inorganic [4] contaminants. Sorption of environmental contaminants to carbon based sorbents represents an important remediation solution [5], but in comparison with activated carbon, carbon based nanomaterials as environmental sorbents are considered relatively new adsorbents of trace pollutants, showing very good potential in future applications [6]. Multiwalled carbon nanotubes (MWCNTs) were investigated for removal of BPA [7], several studies demonstrating their suitability in sorption processes. Their adsorption capacity strongly depends on the surface chemistry, such as the density of surface active sites and the activation energy of the sorption bonds [8]. The transformation of the surface chemistry of MWCNTs depends on the matrices in which these nanostructures appear and on several factors that influence the nature and the number of the functional groups at the surface of MWCNTs. Among these, there are thermal and chemical oxidations and microwave-assisted heating, but also UV irradiation in controlled conditions in synthetic or in environmental media. Several articles [9] treat the impact of UV irradiation over the modification of the surface of MWCNTs, this factor being considered a dominant weathering element known to cause degradation outdoors.

In this study, non-irradiated and irradiated MWCNTs, the last ones assimilated with weathered carbon nanomaterials were studied as adsorbents for BPA, both nanomaterials being characterized before and after the adsorption process. The irradiation experiments were conducted using UV irradiation with the same spectral regime as the UV portion of natural sunlight (300-400 nm), at environmental temperature and humidity. The objectives of our investigation were to compare the characteristics of non-irradiated and irradiated MWCNTs, to evaluate the adsorption capacity of BPA by pristine and irradiated MWCNTs and to determine the variation of the kinetic, sorption and thermodynamic parameters during sorption process using both sorbents.

Experimental part

Materials and methods

Multiwalled carbon nanotubes (MWCNTs) are provided by Baywatch, Germany. Irradiated MWCNTs were prepared in RWTH Aachen, Germany.

Bisphenol A (minimum purity 99 %) was the sorbate selected for this study and it was obtained from Fluka/ Sigma-Aldrich Chemical, Germany. HPLC grade methanol was purchased from VWR Chemicals, France. Stock reference solutions were individually prepared in methanol, and kept in the refrigerator for three months. All working reference solutions were freshly prepared prior to use. Aqueous solutions were prepared using HPLC grade water.

UV irradiated MWCNTs

The experiments were conducted through not-accelerated aging using UV radiation in the UV spectral portion of natural sunlight (300-400 nm), at temperatures of 30-50 ^{0}C and 50-75 % relative humidity. The UV chamber uses a mercury arc lamp system with a uniform UV flux of approx.140 W/m^2, which can contain radiation in the visible range, but with very small impact over the degradation of the MWCNTs. The stability of the light source was carefully controlled during the experiments, no change in radiation intensity being noticed during one month of exposure. The relative humidity and the temperature were controlled using temperature and humidity sensors.

HPLC analytical conditions

HPLC determinations were performed using an Agilent 1100 Series HPLC instrument, with UV-DAD detector and Agilent Chemstation software for data acquisition and analysis. The working parameters of the method were: injection volume: 10µL; run time: 8 min; column temperature: 25^{o}C; column: C18 (Zorbax Eclipse Plus-Agilent), 3.5µm, 100 × 4.6 mm i.d.; flow rate: 0.5 mL/min, isocratic conditions at 80:20 A:B (v/v), where A = methanol and B = HPLC grade water.

* *Phone: 021 4029100*

For the quantification of bisphenol A, an external standard calibration method was used [10] by preparing the standard working solutions from a 1000 mg/L BPA stock solution in water. The calibration curve was constructed by plotting peak area of BPA from the chromatograms of the working standard solutions versus each concentration. The concentration range of the linearity calibration curve was between 10 mg/L and 100 mg/L BPA.

Batch adsorption experiments

The experiments were done at different concentration values of BPA and different concentrations of carbon nanomaterials. The working concentrations of BPA were obtained from a standard solution of 100 mg/L prepared by dilution from the more concentrated 1000 mg/L initial stock solution with distilled water. Each sorption solution was prepared in 100 mL glass vials, by adding 1 mg of adsorbent, weighed at the analytical balance, for each working BPA concentration. All the experiments took place at three different temperatures, 20, 25 and 30 ^{0}C, by stirring the solutions in a thermostatic water bath, at 150 rpm, for 24 hours. The BPA concentrations were determined by the RP-HPLC/UV described method, each 10 minutes of the experiments. The influences of contact time monitored at different concentrations of carbon nanomaterials, of BPA, the influence of *p*H and of the temperature were studied and interpreted.

The BPA rate (%) and adsorption capacity (mg/g) will be calculated by:

$$q = \frac{C_0 - C_x}{m} \times V$$

where q (mg/g) is the BPA adsorption capacity, C_0 (mg/L) and C_x (mg/L) are the initial and equilibrium BPA concentrations in the solution, V (L) is the solution volume and M (g) the mass of adsorbent, respectively.

Characterization of the nanosorbents

BET specific surface areas and pore size distribution

The Brunauer-Emmet-Teller (BET) specific surface area of the samples was determined with a Quantachrome NOVA 2200e instrument. Before each measurement, the samples were degassed at 150°C in vacuum for 4h. The specific surface area was determined from the BET equation and the pore volume from the amount of gas adsorbed at p/p_o = 0.99 [10].

Dispersion characterization using UV-Vis methods

0.01 g/L of non-irradiated and irradiated MWCNTs in 100 mL volumes of mixtures of different ratios CH_3OH:H_2O were prepared. MWCNTs dispersions were sonicated for 30 min, centrifuged and then measured with a GBC Scientific Equipment Pty. Ltd CINTRA 202 V 3749 UV-Vis spectrometer.

Scanning electron microscopy (SEM)

The non-irradiated and irradiated MWCNTs surfaces were studied by SEM: the samples were distributed in thin layers on conductive gold surfaces and the images were taken using a microscope SEM (Philips Quanta Inspect F) coupled with X radiation source of 30 kV and magnification x 2000.

Fourier Transformed Infrared spectrometry (FTIR)

The spectra were done with a FTIR spectrometer Vertex 70 Brucker. These were measured between 4000-400 cm^{-1} with a resolution of 4 cm^{-1}.

Differential scanning calorimetric analysis

Thermal analyses, TG-DSC, of the compounds were carried out with a Netzsch 449C STA Jupiter. Samples were placed in closed Al crucible and heated with 5 K· min^{-1} from room temperature to 550 °C under the flow of 50 mL· min^{-1} Ar. An empty Al crucible was used as reference.

Results and discussions

Characterization of the nanosorbents

The **BET** isotherms obtained through N_2 adsorption at 273 K on the tested nanostructures, showed that weathered MWCNTs present larger pore diameter in comparison with the non-irradiated MWCNTs, with different surface areas, suggesting that by irradiation micropore modifications appeared, hindering the adsorption of N_2 (table 1).

The dispersion of the studied carbon nanotubes in aqueous media was determined by measuring their optical density, at an initial MWCNTs concentration of 0.01 g/L in a ratio of 10:90 (v/v) methanol: water solvent mixtures, at

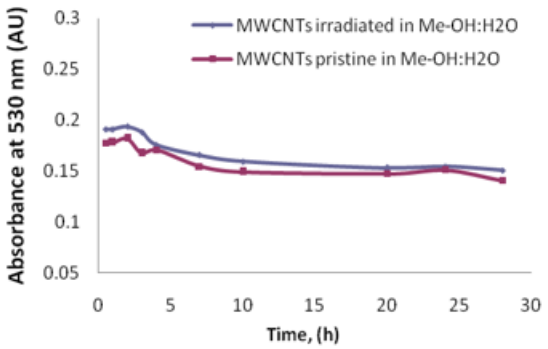

Fig. 1 The absorbance intensities of aqueous suspensions of the studied MWCNTs, over a 28 h period for a methanol: water ratio of 10:90 and a concentration of 0.01 g/L

530 nm, immediately and each 30 min thereafter, over a 28 h period (fig. 1).

The initial optical density was considered as the maximum dispersed mass of the non-irradiated and irradiated carbon nanotubes. It reduced by time during 28 h, and then it remained constant. The optical density at 28 h was considered as a measure of the stability of the suspensions of carbon nanomaterials after settling.

SEM The morphology of the studied MWCNTs, non-irradiated and irradiated before and after sorption of BPA are presented in figure 2. In comparison with pristine MWCNTs, which showed a homogeneous distribution of the nanotubes, the irradiated ones indicate traces on external walls of the nanotubes, corresponding to the oxygen containing functional groups on their surface.

The study of MWCNTs pristine and irradiated by scanning electron microscopy indicates thin films of molecules of BPA on the walls. BPA molecule might interact with the surface of the nanotubes through one hydroxyl group and

Table 1

CHARACTERISTICS OF THE STRUCTURE OF THE NANOMATERIALS USED IN THIS STUDY

Nanomaterial	Purity, %	Specific surface area, m^2/g	Pore volume, cm^3/g	Pore diameter, nm
MWCNTs pristine	95 %	170.77	1.09	3.20
MWCNTs irradiated	95 %	131.55	1.58	1.79

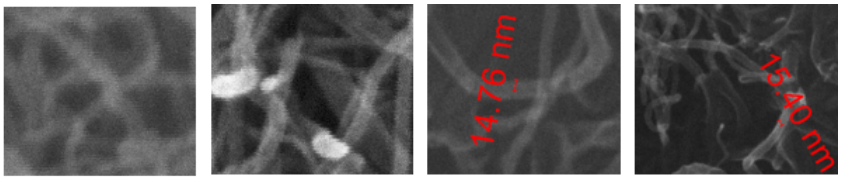

Fig. 2 SEM images of MWCNTs pristine and irradiated, before and after impregnation with BPA: 1-MWCNTs pristine without BPA; 2- MWCNTs pristine with BPA; 3 -MWCNTs irradiated without BPA; 4 -MWCNTs irradiated with BPA

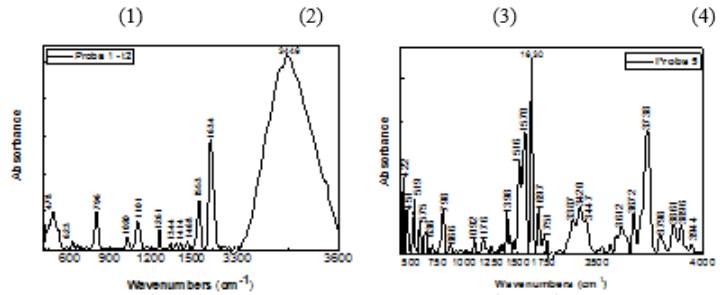

MWCNTs pristine BPA-MWCNTs pristine

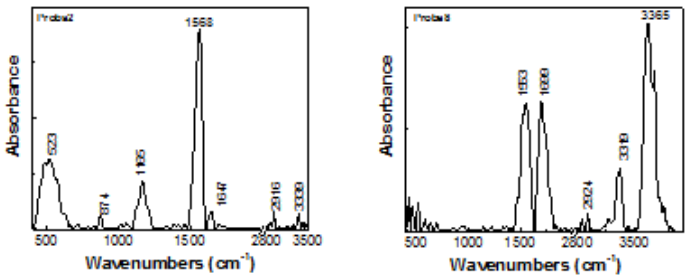

MWCNTs irradiated BPA - MWCNTs irradiated

Fig. 3 FTIR spectra of MWCNTs non-irradiated [11] irradiated before and after sorption of BPA

π-π interaction, or through two hydrogen bonds with both hydroxyl groups, but without π-π interaction [11].

FTIR spectra of the studied nanostructures showed that BPA molecules appeared on the surface of the non-irradiated and irradiated MWCNTs. Irradiated MWCNTs present two specific peaks at 1600 and 3450 cm^{-1}, associated to O-H groups and one corresponding to the benzene rings from the structure of MWCNTs at 1445 cm^{-1}. The functional groups on the surface of the studied MWCNTs appeared at: 3420 cm^{-1} for the stretching vibration of HO- groups; at 1727 cm^{-1} for the C = O double bonds of the carboxylic groups; at 1622 cm^{-1} for the skeleton vibration of C = C double bonds from the benzene ring; at 1380 cm^{-1} for the O = C-O groups, and at 1220 cm^{-1} for the C-O-C groups. In the FTIR spectra of the non-irradiated MWCNTs the peak at 3450 cm^{-1} corresponding to stretching vibration of H-O decreases, and the peaks at 1150 cm^{-1} attributed to the stretching vibration of C-O bond were reduced. The skeleton vibrations of the C = C bond from aromatic nucleus appear at 1633 and 1523 cm^{-1}.

After the BPA adsorption, the spectra indicated the presence of oxygen containing groups at 1200 cm^{-1} for C-OH stretching vibration, at 1700 and 3600 cm^{-1} for the O-H stretching vibration and at 1630 cm^{-1} for the skeleton vibration of the carbon double bond from the aromatic ring, shifted by the presence of the BPA molecules on the benzene rings of the MWCNTs (fig. 3).

Thermal analysis

The thermal stability of MWCNTs, which may present a decomposition process during the sorption process, was analyzed. Experimental results were compared with the literature [12].

It can be observed that pure BPA melted at 155.4 ^{0}C, with a mass loss at 170 ^{0}C and it decomposes at 265.5 ^{0}C, with a mass loss of 79 %, in comparison with the impregnated MWCNTs and irradiated MWCNTs, where the mass loss appears at 310 ^{0}C, probably due to structure modifications of the organic molecule. It also can be noticed that the mass loss of impregnated MWCNTs with BPA is very small, probably the interactions between the organic molecule and the nanomaterial leading to more volatile compounds (figs. 4, 5).

Carbon nanotubes are typically stable at temperatures values up to 600 °C with mass loss of 3-4 %. MWCNTs pristine impregnated with BPA show a mass loss of 8.04 %, at 241 ^{0}C, in comparison with the irradiated ones impregnated with BPA which show a mass loss of 9.04%, at 227^{0}C. Thermal degradation of irradiated MWCNTs is a stepwise process due to various functional groups existing on the surface of the nanostructures. The first mass loss for all analyzed samples occurs at temperatures values less than 200^{0}C, being attributed to nanomaterials

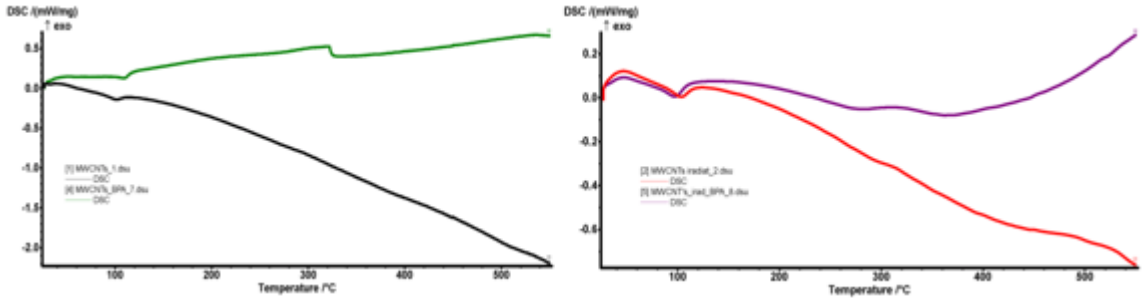

Fig. 4 DSC of pristine MWCNTs and irradiated MWCNTs before and after sorption of BPA

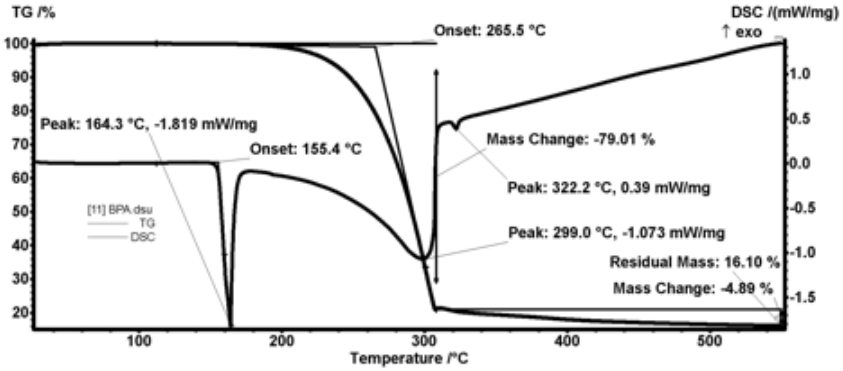

Fig. 5 TGA and DSC of pure BPA, adsorbed BPA on non-irradiated MWCNTs, adsorbed BPA on irradiated MWCNTs

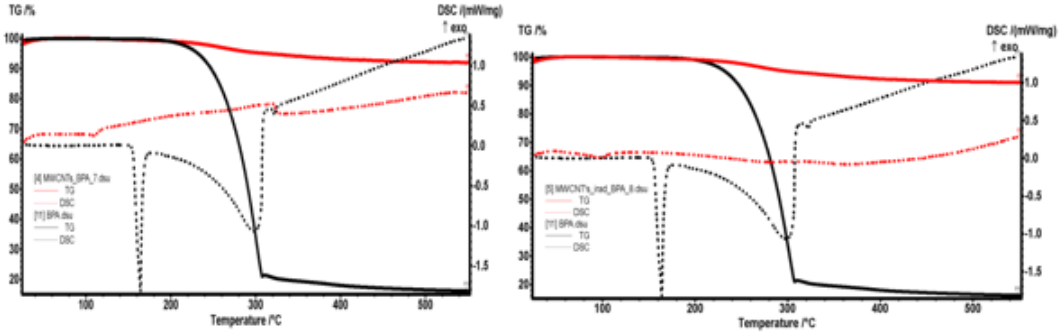

saturation with water vapor and their disposal. At higher values of the temperature, the mass loss may be due to thermal decomposition of the functional groups. DSC analysis indicates that in the case of MWCNTs there is no significant loss of mass between 100 and 200^{0}C, meaning that inclusion water molecules are absent from their crystalline lattice. The thermal stability of MWCNTs can be attributed in the case of MWCNTs to the bonds from aromatic rings, affected by the number of walls of the nanotubes, the nature of the catalyst used in their synthesis and the presence of defects in the material. DSC curves show mass loss at the temperature of 550^{0}C for pristine MWCNTs and at 575^{0}C for irradiated MWCNTs. In the case of carbon nanostructures impregnated with BPA, the temperature rises to 600^{0}C for MWCNTs RWTH and drops to 550^{0}C for irradiated MWCNTs impregnated with BPA.

Kinetic analyses of BPA adsorption on pristine and irradiated MWCNTs

It was observed that the adsorption kinetics of BPA on the studied carbon nanomaterials was limited by diffusion mechanisms: external diffusion, boundary layer diffusion and intra-particle diffusion. The kinetic study was developed at an initial 10 mg/L BPA concentration, at 20 °C and *p*H values between 6-7, in order to determine the adsorption time required to reach the equilibrium. Each 10 min , the concentrations of BPA were measured during three hours. It was observed that the adsorption process is fast (30 min) and the desorption step does not begin during the studied period of time (fig.6).

Pseudo-first and pseudo-second models were applied to the experimental data, to understand the kinetic adsorption process [13, 14]. The mechanisms that govern the adsorption kinetics are mostly based on diffusion (table 2), such as external diffusion boundary, boundary layer diffusion and intra-particle diffusion [15].

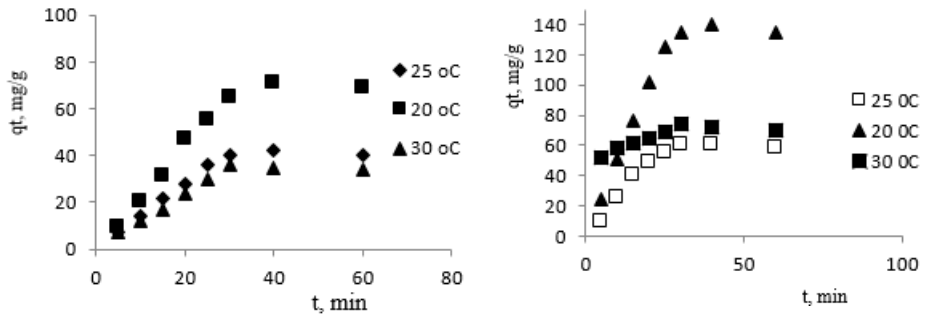

Fig. 6. Kinetics of BPA on non-irradiated (1) and irradiated MWCNTs (2); Conditions: Ci =10 mg/L BPA, T = 25, 20, 35 ^{0}C, V = 100 mL, contact time 3 h

Table 2

KINETIC PARAMETERS FOR THE ADSORPTION OF BPA ON MWCNTs PRISTINE AND IRRADIATED AT 20^{0}C

Sorbent	Pseudo-first order model				Pseudo-second order model		
	q_e, exp, mg/g	k_1, L/min	q_e calc, mg/g	R^2	k_2, mg/g/min	qe calc, mg/g	R^2
MWCNTs pristine	140	0.1233	304.21	0.9266	0.00059	125.0	0.9997
MWCNTs irradiated	171	0.0895	329.33	0.9259	0.00053	180.83	0.7912

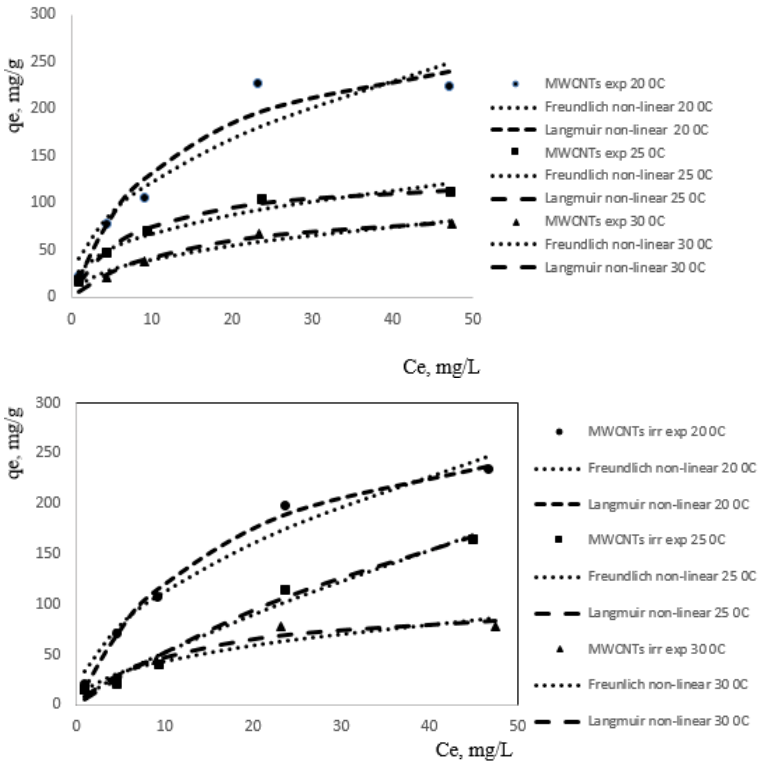

Fig. 7 Adsorption isotherms of BPA on MWCNTs non-irradiated (1) and irradiated (2); Conditions: Ci =10 mg/L BPA, T = 25, 20, 35 ^{0}C, V = 100 mL, contact time 3 h, equilibrium reached after 30 min

BPA adsorption isotherms

This study adopted the Langmuir and Freundlich isotherms to describe the equilibrium adsorption. The Langmuir isotherm assumes monolayer coverage of the adsorption surface without interactions between adsorbed molecules, so when the adsorption saturates no further adsorption occurs (fig. 7). The Freundlich isotherm is derived to model the multilayer adsorption and the adsorption on heterogeneous surfaces [16].

It can be observed from table 3 that the adsorption capacities increased with BPA concentration, the maximum adsorption capacities of pristine MWCNTs being smaller than of the irradiated ones at the same temperature and decreasing by increasing the temperature.

Thermodynamic studies

The thermodynamic parameters offer information over the energetic modifications associated with adsorption (fig. 8). Changes in the enthalpy and entropy of adsorption are connected with the type of adsorption, endothermic or exothermic.

Positive values of ΔH^0, (kJ mol^{-1}) are usually related to chemical reactions and to chemisorption processes. The values obtained in this study reveal that the adsorption on MWCNTs pristine and irradiated might take place by physical sorption (table 4). The negative values of ΔH^0, (kJ mol^{-1}) show also the sorption process on both types of MWCNTs is exothermic in both cases. Since ΔG^0, (kJ mol^{-1}) is negative in connection with the positive values of ΔS^0, (J mol^{-1}K^{-1}) indicate a spontaneous process of adsorption with good affinity for BPA.

Sorption conditions	Langmuir constants			Freundlich constants		
	q_m, mg/g	K_L, L/mg	R^2	K_F	n	R^2
MWCNTs pristine 20 ^{0}C	305.36	0.077	0.9762	42.40	2.18	0.9907
MWCNTs pristine 25 ^{0}C	132.72	0.131	0.9581	28.26	2.65	0.9945
MWCNTs pristine 30 ^{0}C	103.37	0.069	0.9917	14.12	2.20	0.9704
MWCNTs irradiated 20 ^{0}C	353.80	0.013	0.9999	8.57	1.27	0.9720
MWCNTs irradiated 25 ^{0}C	321.58	0.060	0.9897	35.28	1.97	0.9714
MWCNTs irradiated 30 ^{0}C	105.85	0.081	0.9813	16.11	2.29	0.9758

Table 3
ISOTHERM PARAMETERS FOR THE ADSORPTION OF BPA BY MWCNTs PRISTINE AND IRRADIATED AT DIFFERENT TEMPERATURES

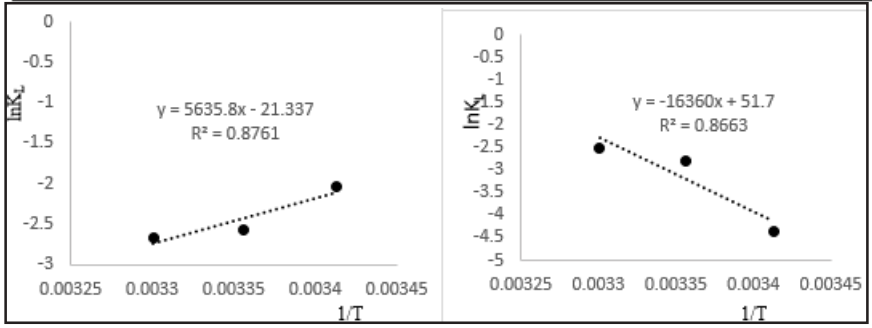

Fig. 8 Plot of Gibbs free energy change *vs.* temperature for the adsorption of BPA on MWCNTs pristine and irradiated

Thermodynamic parameter	ΔH^0, (kJ mol^{-1})	ΔS^0, (J $mol^{-1}K^{-1}$)	ΔG^0, (kJ mol^{-1})		
			293	298	303 K
MWCNTs pristine	- 46.85	17.73	-98.21	-99.70	-100.58
MWCNTs irradiated	- 136.08	42.98	-261.95	-264.10	-266.25

Table 4
THERMODYNAMIC PARAMETERS FOR ADSORPTION OF BPA ON MWCNTs PRISTINE AND IRRADIATED

Effect of pH

An important factor that influences the structure of BPA molecule and its adsorption on the sites of MWCNTs is the *p*H [17]. The *p*H modifies the electrical surface charges of the adsorbent, as well as the dissociation of the adsorbate. Based on the type and functionalization of the carbon nanomaterial and on the values of the dissociation constants (pKa) of the sorbate, the adsorption process in aqueous solutions may develop with the molecular form of the sorbate at *p*H lower than pKa (pKa of BPA = 9.6 - 10.2), or with the deprotonated structure, owing in view that the BPA molecule will lose protons at *p*H above pKa. For *p*H values higher than pKa, the BPA molecules transform themselves in bisphenolate anions ($HBPA^-$ and BPA^{2-}) and present electrostatic repulsion with the negatively-charged sorbent, at these *p*H values. Log K_{ow} is also influenced by the *p*H, the highest values being determined between *p*H 6 and 8. At *p*H values higher the pKa, log K_{ow} decreases because the BPA is not any more in its neutral form.

Adsorption mechanism

Sorption of BPA at the surface of the carbon nanomaterial is driven by hydrophobicity, dispersion and weak polar forces [18]. The improved sorption on carbon based nanosorbents might be explained based on the π-π electron-donor-acceptor (EDA) interactions [19] and on the absence of pore diffusion [20]. Capillarity contributes to the orientation of the sorbate molecules. For pristine or non-irradiated MWCNTs the physical sorption can be considered the dominant mechanism of sorption, rapid equilibrium rates following the traditional Langmuir and Freundlich isotherms [21].

In the case of irradiated MWCNTs (fig. 9), entanglements might appear due to the van der Waals interactions between the ends of the nanotubes [22, 23]. It is also possible that the MWCNTs are increasingly oxidized by the UV irradiation [24]. The MWCNTs entanglement might hinder the dispersion even under sonication treatment [25]. The van der Waals interactions between carbon nanotubes are about 500 eV/μm, explaining the tendency to aggregation.

Some values of the adsorption capacity of BPA by carbon nanotubes already published in the literature are shown in table 5.

Conclusions

Due to it good adsorption capacity, the studied nanomaterials may be considered as alternative adsorbents for removing organic contaminants from water in environmental application. The effects of contact time and of the initial concentration of the adsorbate are compulsory for minimizing the operation time and the efficiency of the treatment process meaning economic benefits to the system. The adsorption capacity of BPA increased by increasing the initial BPA concentration on both pristine and irradiated MWCNTs. This tendency could be explained by a larger driving force provided by the higher BPA concentration, which could defeat the mass transfer resistance between the aqueous and solid phases.

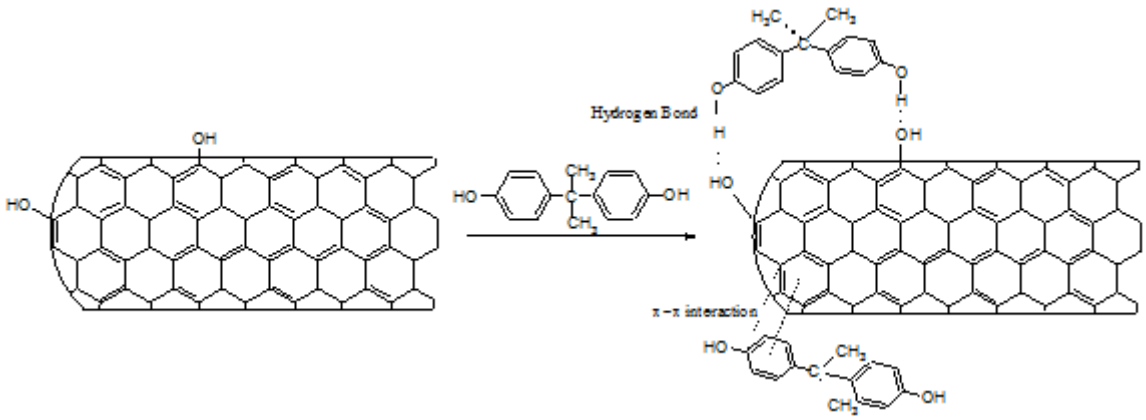

Fig. 9 Mechanism of interaction between carbon nanotubes and BPA

Adsorbent	T (°C)	Sorbent/ solution (w/v) ratios	Contact time	pH	C_s (mg/g)	Reference
SWCNTs (single-walled carbon nanotubes)	20	1 mg/255 mL	one week	-	126.1	3
MWCNTs (multi-walled carbon nanotubes)	20	1 mg/255 mL	one week	-	29.8	3
MWCNTs	27	0.125 g/1L	24 h	6	59.17	1
SWCNTs	20	0.5 g/1L	60 min.	9	71	26
MWCNT	20	0.5 g/1L	60 min.	9	111	26
GO (graphene oxide)	25	10 mg/50 mL	60 min.	3.5	49.26	27
GO	25	10 mg/100 mL	30 min.	6	87.80	28

Table 5
ADSORPTION CAPACITY OF BPA BY CNTs IN COMPARISON TO OTHER LITERATURE VALUES [11]

Acknowledgments: This research was performed in the frame of ERA-NET SIINN, funded by the European Commission within the 7th Framework Program and supported by the Romanian Executive Agency for Higher Education and RDI Funding (Unitatea Executiva pentru Finantarea Invatamantului Superior, Cercetarii, Dezvoltarii si Inovarii: UEFISCDI).

References

1.C.Y. KUO, Desalination, **249**, 2009, p. 976–982
2.RADU, R. STOICA, R., OPRESCU, E., BOLOCAN, I. ION, I., ION, A.C., Rev. Chim.(Bucharest), **67**, no. 2, 2016, p. 230
3.O. G. APUL, Q. WANG, Y. ZHOU, T. KARANFIL, Water Research, **47**, 2013, p. 1648-1654.
4.M.A. SHANNON, P.W. BOHN, M. ELIMELECH, J.G. GEORGIADIS, B. J. MARINAS, A. M. MAYES, Nature, **452**, 2008, p. 301-310.
5.N. SAVAGE, M.S. DIALLO, J. Nanopart. Res., **7**, 2005, p. 331-342.
6M.S. MAUTER, M. ELIMELECH, Environ. Sci. Technol., **42**, nr. 16, 2008, p. 5843-5859.
7. JIYONGHEO, J. R.V. FLORA, N. HER, Y.G PARK, J. CHO, A. SON, Y. YOON, Separation and Purification Technology, **90**, 2012, p. 39–52.
8R.M. ALLEN-KING, P. GRATHWOLL, W.P. BALL, Adv. Water Resources, **25**, 2002 p. 985-1016.
9.T. NGUYEN, E. J. PETERSEN, B. PELLEGRIN, J. M. GORHAM, T. LAM, M. ZHAO, L. SUNG, Carbon, **116**, 2017, p. 191-200.
10.J. ZHAO, Z. WANG, S. GHOSH, B. XING, Environ. Pollut., **184**, 2014, p. 145-153.
11.R.M. SENIN, I. ION, A.C. ION, Pol. Environ. Stud., **27**, nr. 5, 2018, p. 1-13.
12.C.-P. LIN, J.-Z. LIN, C.-M. SHU, J.-M. TSENG, J. LOSS, Prevention Process Ind., **25**, 2012, p. 302-308.
13.G. BLANCHARD, M. MAUNAYE, G. MARTIN, Water Res., **18**, 1984, p. 1501-1507.
14.W. J. WEBER, J.C. MORRIS, J. SANIT, Eng. Div. ASCE, **89**, 1963, p. 31-59.
15.E. GUIBAL, P. MCCARRICK, J.M. TOBIN, Sep. Sci. Technol., **38**, 2003, p. 3049-3073.
16. A.C.ION, I. ION, A. CULETU, Mat. Sci. Eng. B, **176**, 2011, p. 504-509.
17. S. BORRIRUKWISITAK, H.E. KEENAN, C. GAUCHOTTE-LINDSAY, International J. Environ. Sci. Development, **3**, nr. 5, 2012, p. 460-464.
18. W. CHEN, L. DUAN, D. Q. ZHU, Environ. Sci. Technol., **41**, 2007, p. 8295-8390.
19. R.Q. LONG, R.T. YANG, J. Am. Chem. Soc., **123**, 2001, p. 2058-2059.
20. S. GOTOVAC, Y. HATTORI, D. NOGOGUCHI, J. MIYAMOTO, M. KANAMARU, S. UTSUMI, H. KANOH, K. KANEKO, J. Phys. Chem. B, **110**, 2006, p. 16219-16224.
21. X.J. PENG, Y.H. LI, Z.K. LUAN, Z.C. DI, H.I. WANG, B.H. TIAN, Z.P. JIA, Chem. Phys. Lett., **376**, 2003, p. 154-158.
22. F. VARGAS-LARA, J.F. DOUGLAS, Soft Matter, **11**, nr. 24, 2015, p. 4888-4898.
23. W. LU, T.-W. CHOU, J. Mech. Phys. Solids, **59**, nr. 3, 2011, p. 511-524.
24. E.J. PETERSEN, T. LAM, J.M. GORHAM, K.C. SCOTT, C.J. LONG, D. STANLEY, Carbon, **69**, 2014, p. 194-205.
25. L. A. GIRIFALCO, M. HODAK, R.S. LEE, Phys. Rev. B Condens. Matter, **62**, nr.19, 2000, p. 13104-13110.
26. M. H. DEHGHANI, A. H. MAHVI, N. RASTKARI, R. SAEEDI, S. NAZMARA, E. IRAVANI, Desalination and Water Treatment, **54**, 2015, p. 84–92.
27. T. PHATTHANAKITTIPHONG, G. T. SEO, Nanomaterials, **6**, 2016, p. 128.
28. X. JING, Z. Y. FA, Acta Physico-Chimica Sinica, **29**, nr. 4, 2013, p. 829-836.

Manuscriptreceived: 3.08.2017